Enhanced performance of dicationic ionic liquid electrolytes by organic solvents

2014 J. Phys.: Condens. Matter 26 284105

(http://iopscience.iop.org/0953-8984/26/28/284105)

IOP Publishing Journal of Physics: Condensed Matter
J. Phys.: Condens. Matter **26** (2014) 284105 (9pp) doi:10.1088/0953-8984/26/28/284105

Enhanced performance of dicationic ionic liquid electrolytes by organic solvents

Song Li[1], Pengfei Zhang[2], Pasquale F Fulvio[2], Patrick C Hillesheim[2], Guang Feng[1, 4, 5], Sheng Dai[2, 3] and Peter T Cummings[1]

[1] Department of Chemical and Biomolecular Engineering, Vanderbilt University, Nashville, TN 37235, USA
[2] Chemical Sciences Division, Oak Ridge National Laboratory, Oak Ridge, TN 37831, USA
[3] Department of Chemistry, University of Tennessee, Knoxville, TN 37996, USA
[4] State Key Laboratory of Coal Combustion, Huazhong University of Science and Technology, Wuhan 430074, People's Republic of China
[5] School of Energy and Power Engineering, Huazhong University of Science and Technology, Wuhan 430074, People's Republic of China

E-mail: guang.feng@vanderbilt.edu

Received 19 November 2013, revised 7 February 2014
Accepted for publication 10 February 2014
Published 12 June 2014

Abstract

The use of dicationic ionic liquid (DIL) electrolytes in supercapacitors is impeded by the slow dynamics of DILs, whereas the addition of organic solvents into DIL electrolytes improves ion transport and then enhances the power density of supercapacitors. In this work, the influences of organic solvents on the conductivity of DILs and the electrical double layer (EDL) of DIL-based supercapacitors are investigated using classical molecular dynamics simulation. Two types of organic solvents, acetonitrile (ACN) and propylene carbonate (PC), were used to explore the effects of different organic solvents on the EDL structure and capacitance of DIL/organic solvent-based supercapacitors. Firstly, it was found that the conductivity of DIL electrolytes was greatly enhanced in the presence of the organic solvent ACN. Secondly, a stronger adsorption of PC on graphite results in different EDL structures formed by DIL/ACN and DIL/PC electrolytes. The expulsion of co-ions from EDLs was observed in DIL/organic solvent electrolytes rather than neat DILs and this feature is more evident in DIL/PC. Furthermore, the bell-shaped differential capacitance–electric potential curve was not essentially changed by the presence of organic solvents. Comparing DIL/organic solvent electrolytes with neat DILs, the capacitance is slightly increased by organic solvents, which is in agreement with experimental observation.

Keywords: dicationic ionic liquids, organic solvents, electrical double layer, capacitance

S Online supplementary data available from stacks.iop.org/J.Phys/26/284105/mmedia

(Some figures may appear in colour only in the online journal)

1. Introduction

Room temperature ionic liquids (RTILs) are being employed as safe and green electrolytes in electric double-layer capacitors (EDLCs) or supercapacitors with ultrahigh energy density [1–3]. At present, the majority of RTILs under investigation are monocationic ionic liquids (MILs) carrying a single unit charge in each cation. The emergence of germinal dicationic ionic liquids (DILs) is attracting increasing interest in research due to their high electrochemical stability [4]. In general, the glass transition temperature of DILs is higher compared with that of their monocationic counterparts [5]. Thus, DILs are more viscous, which greatly restricts their successful application as electrolytes for high power density supercapacitors. To overcome the relative high viscosity, organic solvents such as acetonitrile (ACN), propylene carbonate (PC) and

acetone are commonly used as additives of RTILs to improve their conductivity [6, 7] as electrolytes for supercapacitors [8–10], batteries [11, 12] and solar cells [13]. PC was reported to exhibit a higher density, viscosity and dielectric constant than ACN [20]. It also displays a slightly stronger polarity in contrast to ACN. However, ACN was found to be the most suitable solvent of RTILs for carbon-based supercapacitors since ACN/RTIL electrolytes exhibit less electric resistance and nearly constant energy density with the increase of power density [8]. For instance, Chaban *et al* reported that the ionic conductivity of RTILs was increased more than 50 times by the addition of ACN with high diffusion coefficients and low viscosity using molecular dynamics (MD) simulation [14]. Experimentally, the excellent capacitive performance of DILs in contrast to MILs was solely observed in cyclic voltammetry at an extremely slow scan rate [15], whereas the addition of ACN or PC into DILs favors the higher capacitance of DILs over the counterpart MILs even at a high scan rate (400 mV s^{-1}) [10].

Although the influence of organic solvents on the electric double layer (EDL) of MILs near the carbon electrode has been reported [16–19], the molecular insight into the EDLs formed by DIL/organic solvents near the carbon electrode is still elusive. Merlet *et al* reported that the organic solvent ACN reduced the layering of MILs in EDLs, facilitated the dissociation of cation–anion pairs and attenuated the dissymmetry between positive and negative potentials [17]. The capacitance of ACN/RTIL-based electrolytes in supercapacitors was slightly increased compared with neat RTIL-based supercapacitors in MD simulations [18], whereas the density function theory revealed an enhanced capacitance in carbon nanoslits once the organic solvents were involved [19]. However, despite the benefits of using ACN as a solvent for RTILs, the influence of the ACN solvent on the capacitance of DIL-based supercapacitors, especially on the shape of the differential capacitance–electric potential (*C*–*V*) curves, is poorly understood.

In this work, classical MD simulation was employed to investigate the conductivities of a DIL (1-hexyl-3-dimethylimidazolium bis(trifluoromethyl)imide) $[C_6(mim)_2](Tf_2N)_2$ in ACN at varying concentrations as well as the EDL structures and *C*–*V* curves for neat $[C_6(mim)_2](Tf_2N)_2$ and $[C_6(mim)_2](Tf_2N)_2$/organic solvent mixture at a planar graphite electrode. Considering the different physiochemical properties and chemical compositions of PC and ACN, there is great interest in studying their interfacial behavior at the graphite electrode. Therefore, both ACN and PC were adopted as solvents in this study in order to probe the effects of different organic solvents on the EDLs formed by DILs at graphite electrodes. Experimental measurement of the conductivity of $[C_6(mim)_2](Tf_2N)_2$ in ACN solution is performed as well. Different shapes of *C*–*V* curves were expected for neat DIL and DIL/organic solvent-based supercapacitors.

2. Methodology

2.1. DIL synthesis and conductivity measurement

DIL $[C_6(mim)_2](Tf_2N)_2$ was prepared through intermediate $[C_6(mim)_2](Br)_2$ according to the protocol described in [4]. Initially, 15.0 ml (0.098 mol) of 1,6-dibromohexane was added into 15.6 ml (0.196 mol) of 1-methylimidazole with 20 ml CH_3CN solvent drop by drop under argon flowing at room temperature. The reaction was then heated to 60 °C for 8 h and the organic solvent was subsequently removed under reduced pressure, affording crude $[C_6(mim)_2](Br)_2$. The bromide salt was dissolved in 100 ml water and then extracted with three 25 ml aliquots of ethyl acetate. The remaining water was removed by heating under a vacuum and then ion exchange was performed using $[C_6(mim)_2](Br)_2$ and $LiTf_2N$ in water to yield $[C_6(mim)_2](Tf_2N)_2$. $[C_6(mim)_2](Tf_2N)_2$ was separated and then freeze-dried for three days.

All the chemicals were of AR grade. They were commercially purchased from Sigma Aldrich and used without further treatment.

The IL solutions were prepared under an argon atmosphere and using ACN (Sigma Aldrich) as a solvent. All measurements were taken at 25.0 °C using a two-electrode cell and a Gamry potentiostat. The conductivity values were then referenced to a standard 0.100 mol kg^{-1} KCl (aqueous solution) with conductivity at 25.0 °C of 0.0128 S cm^{-1} (the resistivity of the standard 0.100 mol kg^{-1} KCl at 25.0 °C was 96.00 Ω).

2.2. Simulation setup

The parameters for $[C_6(mim)_2]^{2+}$ were adapted from the all-atom force field developed by Yeganegi *et al* [21]. The force field of $[Tf_2N^-]$ was taken from the study of Lopes *et al* [22]. The new six-site model was used for the simulation of ACN [23], which has been successfully used to model the mixture of ILs and ACN [14]. All the parameters for PC in the MD simulation were taken from the generalized Amber force field (GAFF) [24] with optimized partial charges obtained from the work of Yang *et al* [25]. The van der Waals interaction parameters for carbon of the graphite electrode were taken from the study of Cornell *et al* [26]. All the C–H bonds were constrained during the simulation using the LINCS algorithm [27] and a 1.1 nm cutoff was used for van der Waals interactions. Long-range electrostatic interactions were treated using the particle mesh Ewald method [28] with correction for slab geometry [29, 30]. The periodic boundary condition was applied in three dimensions. A distance of 7 nm between the positively and negatively charged graphite was applied with a vacuum space of 28 nm in length between the simulation cells. All simulations were performed in a modified version of the MD package Gromacs [31]. The three-layer graphite electrode with a size of 4.18 nm × 4.25 nm was fixed during the simulation. The density of electrolytes in the central portion of a planar graphite cell was tuned to the bulk density. The equilibration was performed in the canonical ensemble at 300 K for 10 ns after annealing from 1000 to 300 K. All the production runs were then conducted at 300 K. The ensemble temperature was controlled by the Nosé–Hoover thermostat, which is frequently used for precise temperature control in MD simulation. The time step of 2 fs was applied and the trajectory was saved every 100 fs for computing the number and charge density profiles. A 6 ns production run generated at 300 K was used for further analysis. Different electric

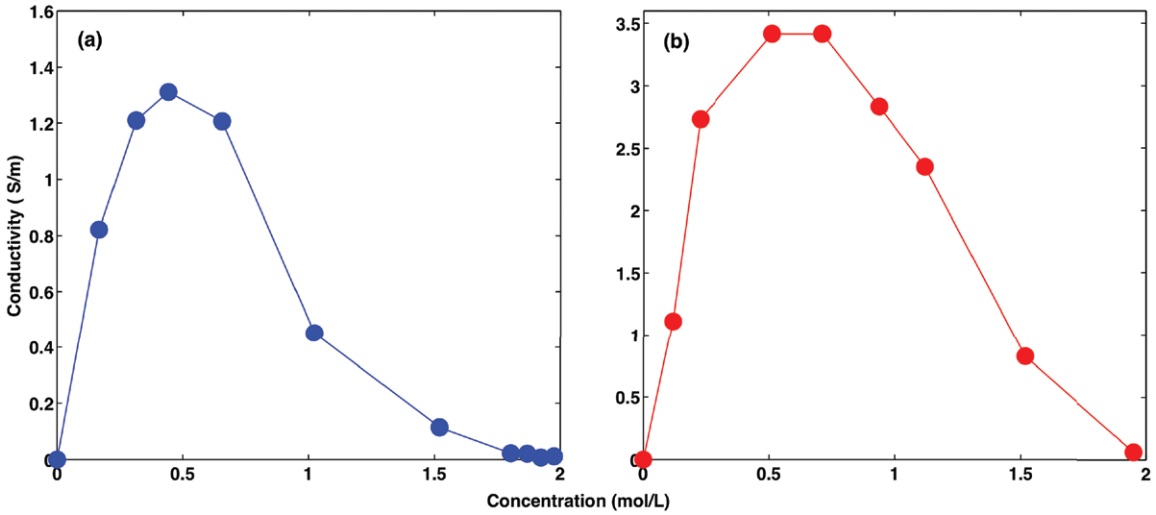

Figure 1. Conductivity of $[C_6(mim)_2](Tf_2N)_2$ as a function of molar concentration in ACN solvent obtained from MD simulations (*a*) and experimental measurement (*b*).

potentials were created by partial charge uniformly distributed on the graphite layer in contact with electrolytes at varying charge densities. The potential drop was calculated using the Poisson equation as in the previous study [18]. The differential capacitance–electric potential (*C*–*V*) curve is obtained by fitting the surface charge density versus electric potential using the fifth-order polynomials. The conductivity of the IL mixture $[C_6(mim)_2](Tf_2N)_2$/ACN is derived from the slope of mean square displacement of the translational dipole moment as stated in the work of Schröder *et al* [31]. The energy density of supercapacitors is calculated using the following equation:

$$E = \frac{1}{2} C_{\text{int}} V_t^2,$$

where C_{int} is the integral capacitance and V_t is the total potential drop between positively and negatively charged electrodes.

3. Results and discussion

The conductivity enhancement of ILs by the organic solvent ACN was firstly investigated by both MD simulation and experimental measurement, as shown in figure 1. It is obvious that the conductivity of the $[C_6(mim)_2](Tf_2N)_2$/ACN solution exhibits a DIL-concentration dependence. With the decrease of the DIL concentration, the conductivity is dramatically increased until it reaches a limiting concentration, below which conductivity reduction is observed due to the smaller number of ions present in the solution, which was evidenced in both the MD (figure 1(*a*)) and experimental measurement (figure 1(*b*)). The highest conductivity of $[C_6(mim)_2](Tf_2N)_2$/ACN is observed at the concentration of 0.5 mol l^{-1}, which is approximately 50 times higher than that of neat $[C_6(mim)_2](Tf_2N)_2$. Conductivity enhancement for MIL/ACN has been reported in another MD simulation [14], in which a similar trend was observed. In addition, the diffusions of both cations and anions were also dramatically increased by ACN (figure S1) (stacks.iop.org/J.Phys/26/284105/mmedia). Our previous study has demonstrated that the outperformance of the DIL in contrast

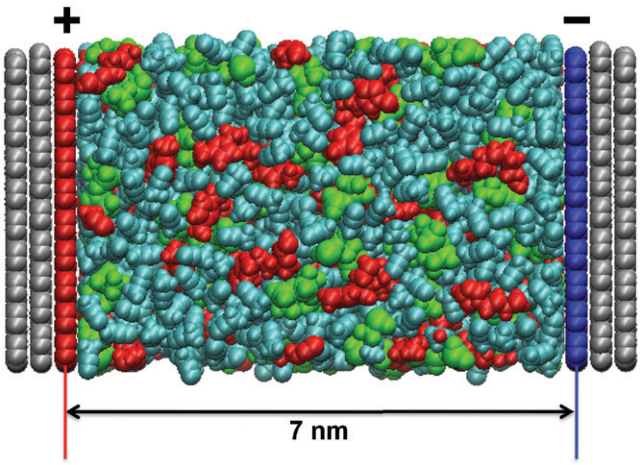

Figure 2. Simulation setup for a supercapacitor cell consisting of two opposite triple layers of graphite with uniformly distributed positive and negative charges on the innermost layers. The red, green and cyan spheres represent cations, anions and organic solvent molecules between two electrodes, respectively.

to the MIL electrolyte in supercapacitors can only be observed at low scan rates [32], which suggests the determining role of dynamic properties of electrolytes. Consequently, the increased diffusion of DILs in ACN indicates the better capacitive performance of DIL electrolytes at high scan rates, thus leading to enhanced power density.

To investigate the capacitive performance of neat DIL, DIL/ACN and DIL/PC electrolytes (5% DILs in molar ratio), respectively, the three electrolytes were employed in graphite-based supercapacitors. The simulation model for supercapacitors is shown in figure 2. The distance between the two electrodes was 7 nm, which is sufficiently distant for electrolytes in the middle to exhibit bulk-like behavior. Once the innermost layers were uniformly charged with opposite charges, an electric potential was applied along the normal direction of graphite, resulting in a densely packed adsorbed layer consisting mostly of counter-ions and a small number

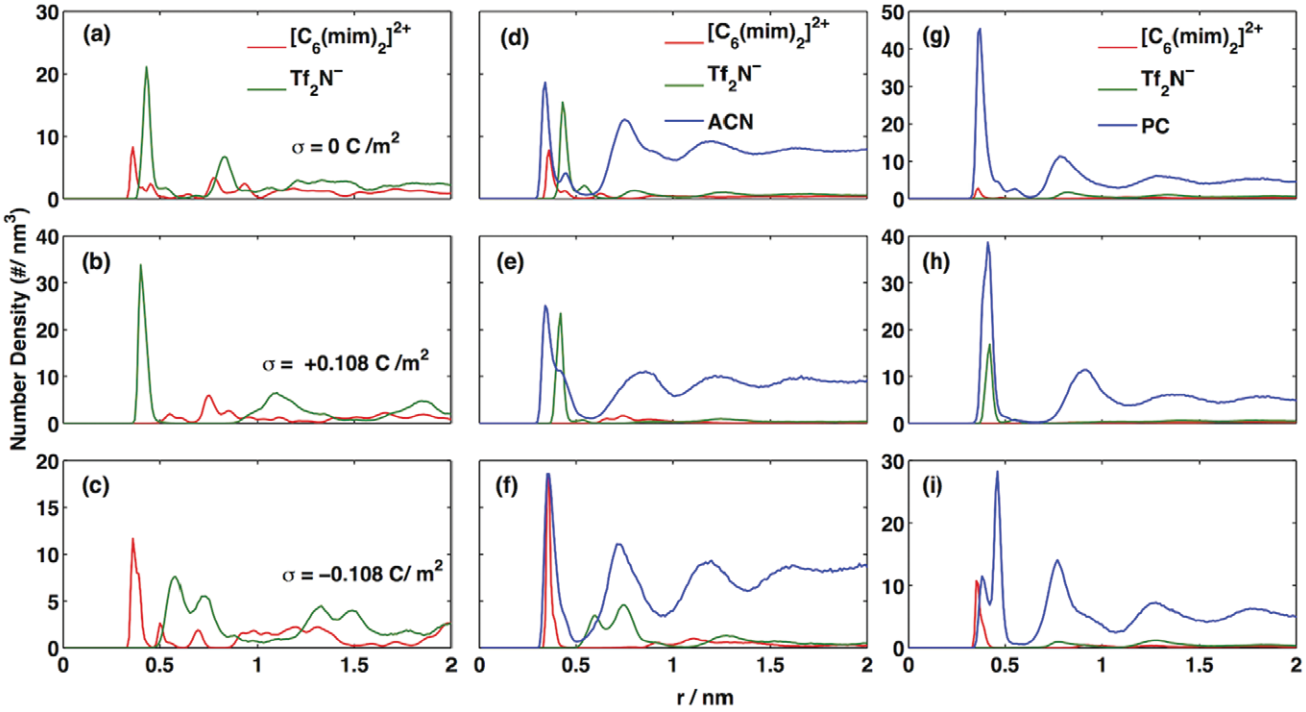

Figure 3. Number density profiles for cations, anions, ACN and PC molecules at uncharged and charged graphite electrodes. The left panels (*a*), (*b*), (*c*) are the number density profiles for neat DIL $[C_6(mim)_2](Tf_2N)_2$. The middle panels (*d*), (*e*), (*f*) and right panels (*g*), (*h*), (*i*) are the number density profiles for $[C_6(mim)_2](Tf_2N)_2$/ACN and $[C_6(mim)_2](Tf_2N)_2$/PC at a molar ratio of 5%.

of co-ions. This adsorbed layer is called an EDL, and is the key to determining the energy storage density in supercapacitors. The effects of organic solvents on the structures of EDLs formed by three electrolytes near neutral and charged electrode surfaces were analyzed and are shown in figure 3.

Comparing the ion density of neat $[C_6(mim)_2](Tf_2N)_2$ with that of $[C_6(mim)_2](Tf_2N)_2$/ACN and $[C_6(mim)_2](Tf_2N)_2$/PC at uncharged/charged electrodes, the layering of ions in neat DIL is more pronounced and more ions of neat DILs are accumulated near electrodes than those of DIL/ACN or DIL/PC. At the charged electrode, fewer counter-ions are present in the EDLs of DIL/ACN and DIL/PC in contrast to those of neat DILs, indicating decreased charge compensation. It was found that the presence of ACN or PC caused the strong expulsion of co-ions from EDLs. A similar phenomenon was reported in an MD study of MIL/ACN electrolyte-based supercapacitors [17]. The expulsion of co-ions is probably because of the weakened cation–anion coupling and/or reduced electrode–ion interaction in IL/ACN due to the presence of polar solvents compared with that in neat IL, leading to the lower energy barrier for co-ions to move away from the electrode surface. The decreased free energy between the electrode and ions in IL/ACN was verified in the study of Merlet *et al* [17]. The calculated coordination number at the interface, i.e. the coordination number of anions surrounding cations located within the first adsorbed layer ($r = 0.0$–0.6 nm), was 4.75 for neat DILs and 2.19 for DIL/ACN, suggesting that ACN molecules facilitate the dissociation of ion pairs, similar to a previous investigation [17]. Therefore, ACN not only weakens the electrode–ion interaction but also enhances the dissociation of cation–anion pairs in the adsorbed layer near the electrode surface.

On the other hand, when comparing the influences of ACN and PC on the EDL structures, it is found that there is a large number of PC molecules adsorbed on the graphite in contrast to ACN. The expulsion of co-ions from EDLs becomes more evident in PC-containing electrolytes. The calculated coordination number of anions surrounding cations in the EDL formed by $[C_6(mim)_2](Tf_2N)_2$/PC is close to 1.20, in contrast to 2.17 for $[C_6(mim)_2](Tf_2N)_2$/ACN. This large discrepancy is attributed to the dissimilar interaction potentials of ACN/graphite and PC/graphite. The interaction potential energy, shown in figure 4, suggests that there is a stronger attraction between PC molecules and graphite compared with ACN/graphite, which leads to a significant accumulation of PC on the graphite. It is also observed that for DIL/PC electrolytes, cations are more preferably adsorbed on graphite rather than anions; for DIL/ACN electrolytes, the difference between the interactions of cation–graphite and anion–graphite is less evident, which coincides with their number density profiles shown in figures 3(*d*) and (*g*).

Moreover, to disclose more details of the interfacial structure of EDLs, the orientational order parameter of ACN and PC near charged/uncharged graphite surfaces was calculated using $\langle P_2 \rangle = \frac{1}{2}(3\cos^2(\theta) - 1)$, as shown in figure 5. The orientational order parameter describes the distribution of angles formed by the surface normal of graphite and the vector pointing from the C atom of the methyl group to the N atom in ACN, as well as those formed by the surface normal of graphite with the plane determined by two O atoms and one C atom between the five-member ring in PC. The results show that ACN in the first adsorbed layer is preferable to parallelize with the graphite surface, which is not obviously influenced by the presence

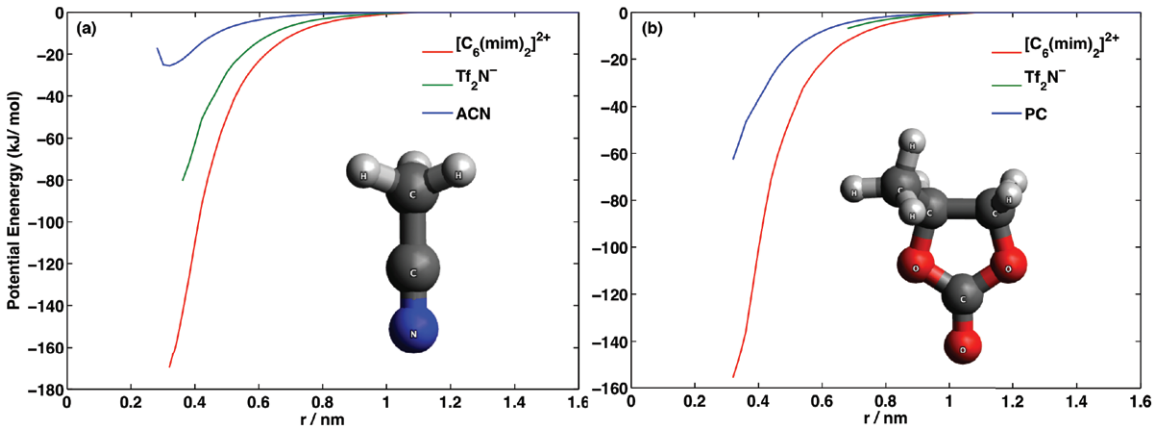

Figure 4. Comparison of averaged interaction potential energy per molecule as a function of distance from the electrode for (*a*) $[C_6(mim)_2](Tf_2N)_2$/ACN and (*b*) $[C_6(mim)_2](Tf_2N)_2$/PC between ions/organic solvents and the neutral graphite electrode. Light and dark gray spheres represent hydrogen and carbon, respectively. Blue spheres represent nitrogen and red spheres represent oxygen atoms.

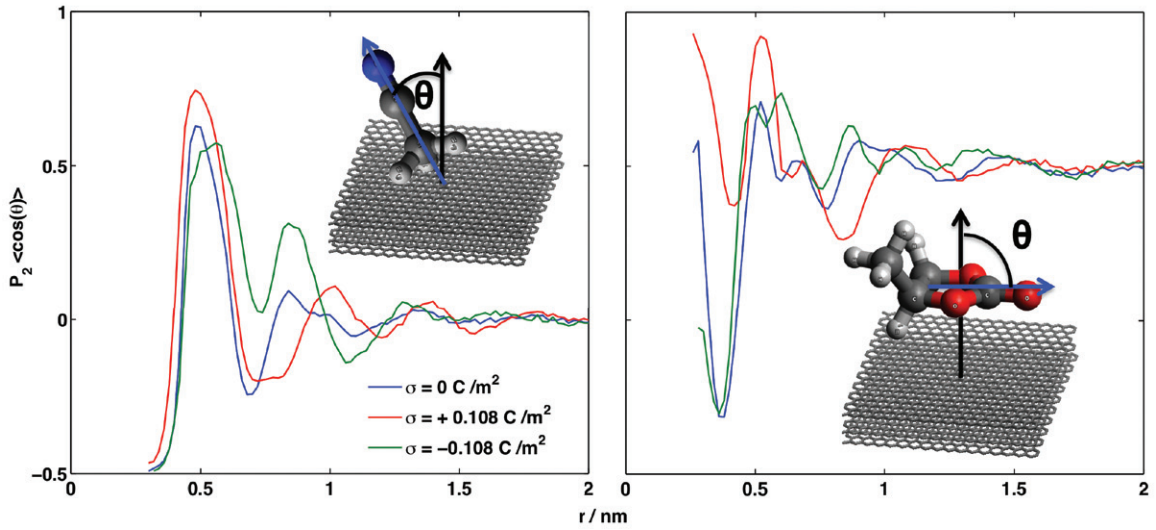

Figure 5. Orientational order parameter of angles formed by the surface normal of graphite with the vector shown in ACN (*a*) and the plane of PC (*b*) as a function of distance to the graphite surfaces.

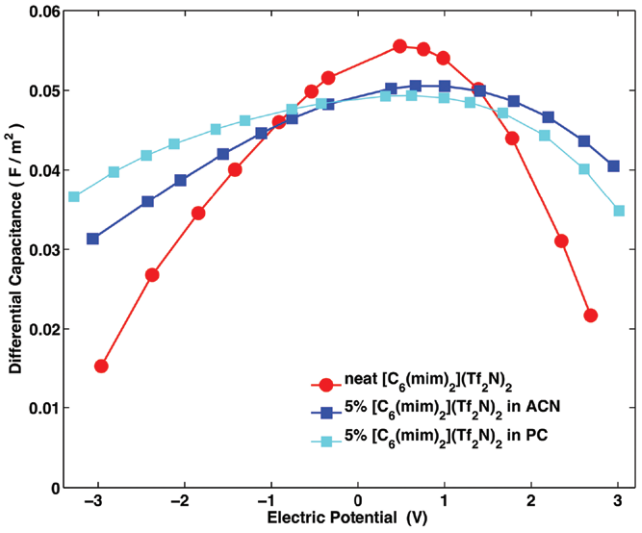

Figure 6. (*a*) Differential capacitance as a function of electric potential applied for neat dicationic $[C_6(mim)_2](Tf_2N)_2$, $[C_6(mim)_2](Tf_2N)_2$/ACN and $[C_6(mim)_2](Tf_2N)_2$/PC electrolytes at the IL ratio of 5%.

of surface charges. However, the orientation of PC molecules on the graphite surface is more sensitive to the surface charge. They tend to tilt at an angle of 50° and 35° with the graphite surface at the neutral and negatively charged graphite, respectively, and as the electrode is positively charged, PC becomes vertically oriented to the graphite surface. This indicates an evident reordering of PC molecules on graphite with the variation of surface charges due to the complicated structure and large size of PC compared with the linear smaller-sized ACN.

The orientations of dications in DIL/ACN, DIL/PC and neat DILs were also compared (figure S2) (stacks.iop.org/J.Phys/26/284105/mmedia). The imidazolium ring of dications in neat DIL in the first adsorbed layer tended to parallelize to the neutral electrode surface, whereas the dications in its neighboring region were found to be perpendicular to the electrode surfaces. The well-ordered organization of dications in the adsorbed layers was not influenced by the presence of ACN or PC, which can probably be attributed to the stronger interaction between electrodes and dications in comparison with anions and ACN or PC (figure 4). At the negatively

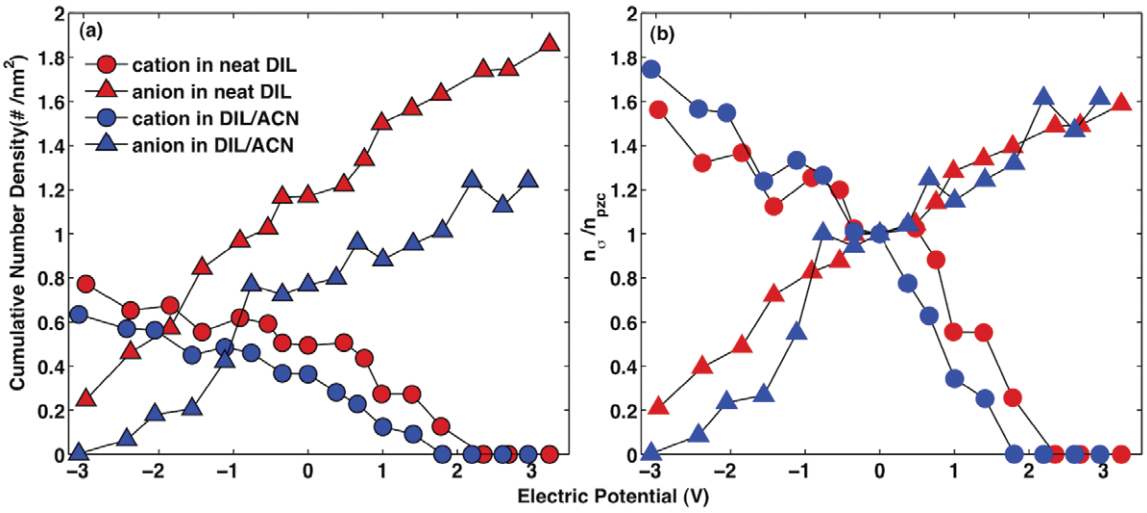

Figure 7. (*a*) Cumulative number density of cations and anions in the EDL as a function of electric potential applied for neat dicationic $[C_6(mim)_2](Tf_2N)_2$ and $[C_6(mim)_2](Tf_2N)_2$/ACN solution at the IL ratio of 5%; (*b*) the ratio of the ion number in EDLs near charged electrodes to that at PZC or the neutral electrode.

charged electrode, the dominant Coulomb interaction between electrodes and counter-ions re-orientates the dications in order to efficiently overcompensate the surface charges on the electrode, which is almost not affected by the presence of ACN or PC.

Then, how will organic solvents influence the *C–V* curve? Merlet *et al*'s coarse-grained MD simulation has revealed that the organic solvent ACN attenuated the dissymmetry of *C–V* curves obtained from neat MIL-based supercapacitors [17]. In this study, such a trend is not observed, probably due to the different ions and ion models (all-atom model versus coarse-grained model) used, since the BF_4-containing IL used in their study is usually accompanied with an asymmetric *C–V* curve. For dicationic $[C_6(mim)_2](Tf_2N)_2$ adopted herein, a typical bell-shaped *C–V* curve is exhibited (figure 6), similar to reported results for MILs [33]. Although the bell-shaped *C–V* curve is not altered by the presence of the organic solvent ACN, the bell curve is flattened, which means that the decrease in the differential capacitance with the increase of electric potential is slowed down. In addition, the overall differential capacitance throughout the potential range is increased by 15% in contrast to neat $[C_6(mim)_2](Tf_2N)_2$ (0.039 F m^{-2} for neat DIL and 0.045 F m^{-2} for DIL/ACN), in agreement with a previous report for MIL/ACN [17].

Although PC exhibits stronger adsorption on graphite and a more obvious expulsion of co-ions from the EDL, DIL/PC displays almost the same shape of *C–V* curve as DIL/ACN with the exception of a slight rise at negative potentials and a subtle decrease at positive potentials. The overall differential capacitance throughout the potential range is very similar to that of DIL/ACN (0.044 F m^{-2} for DIL/PC versus 0.045 F m^{-2} for DIL/ACN). Further explanation is provided later in this paper.

The cumulative number density per unit surface area of electrode (figure 7(*a*)) also provides molecular insight into the enhanced capacitance by the presence of ACN. More concentrated ions in the EDLs of neat DIL than in those of DIL/ACN are observed at both positive and negative potentials. The expulsion of co-ions from EDLs of DIL/ACN is clearly demonstrated in figure 7(*a*), in which the number of co-ions in EDL decreases more rapidly than those of neat DIL with the increase in potential. The depletion of co-ions with increasing potential is inspected for both neat DIL and DIL/ACN; however, the depletion for DIL/ACN is achieved at a lower potential than that for neat DIL, indicating the favorable co-ion expulsion in the presence of ACN. Figure 7(*b*) shows the cumulative number density normalized by the density at potential of zero charge (PZC) or the neutral electrode, n_σ / n_{PZC}, as a function of potential reveals the different change rates of cumulative number densities for counter-ions and co-ions with the variation of electric potential.

At positive potentials, the n_σ / n_{PZC} of counter-ions (anions) increases with increasing potential in order to compensate the surface charges of the electrode; the n_σ / n_{PZC} of co-ions (cations) in DIL/ACN is decreased from 1 at PZC to 0 at ~1.8 V, whereas that in neat DIL starts to decrease from 1 at approximately 0.5 V to 0 at 2.4 V. At negative potentials, counter-ions (cations) exhibit a higher increase rate for DIL/ACN in contrast to neat DIL; the number of co-ions (anions) in DIL/ACN is reduced more quickly from −0.8 V than that in neat DIL and the depletion of co-ions is only observed in DIL/ACN at −3.0 V. At both positive and negative potentials, the quantity of co-ions in EDL is smaller than that in neat DIL. In addition, the number of co-ions decreases faster with increasing potential in DIL/ACN due to the facilitated dissociation of ion pairs in the presence of ACN, indicating that the slightly increased capacitance in DIL/ACN-based supercapacitors can be most probably ascribed to the strong expulsion of co-ions from EDLs.

Another interesting observation is that cations as co-ions are depleted at lower absolute values of potential than anions for both neat DIL (+2.4 V for cations versus < −3 V for anions) and DIL/ACN (+1.8 V for cations versus −3.0 V for anions). This is probably attributable to the concentrated charge

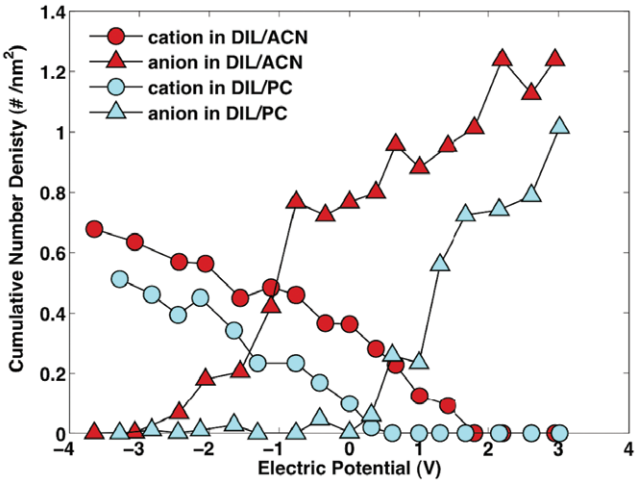

Figure 8. Comparison of the cumulative number density of cations and anions in the EDL as a function of electric potential applied for $[C_6(mim)_2](Tf_2N)_2$/ACN and $[C_6(mim)_2](Tf_2N)_2$/PC solutions at the IL ratio of 5%.

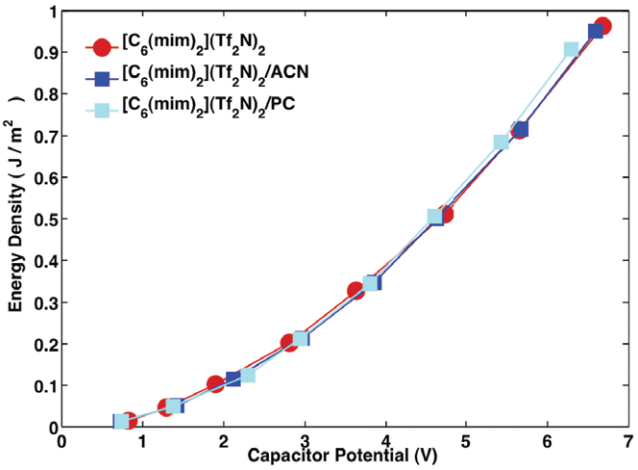

Figure 9. The energy density of capacitors as a function of potential difference between two electrodes for neat $[C_6(mim)_2](Tf_2N)_2$, $[C_6(mim)_2](Tf_2N)_2$/ACN and $[C_6(mim)_2](Tf_2N)_2$/PC electrolytes.

density and bulky size of dications, which associate with two anions. With the increasing electric potential, the repulsion between the positively charged electrode and dications becomes stronger than that between the negatively charged electrode and anions, because the charges in dications are twice those in anions. Moreover, dications with a size nearly twice that of anions (258 Å^3 in volume size for dicationic $[C_6(mim)_2]^{2+}$ and 148 Å^3 for Tf_2N^-) occupy more space in EDLs. In order to effectively screen the positive charges on electrodes, more and more anions were accumulated in EDLs, leading to overscreening or overcompensation of counter-charges on electrodes. Eventually, the number of anions in the EDLs of positively charged electrodes is more than twice that of dications in the EDLs of negatively charged electrodes at the same absolute values of potential (e.g. the number of anions in EDLs is 1.75 at +2.4 V and the number of cations is 0.65 at −2.4 V), which means that more space for anions is required at the positively charged electrode. Therefore, dications as co-ions are favorable to be expelled from EDLs at positive potentials compared with anions at negative potentials, which may be a feature of DILs.

Comparison of the cumulative number densities of cations and anions in EDLs formed by $[C_6(mim)_2](Tf_2N)_2$/ACN and $[C_6(mim)_2](Tf_2N)_2$/PC is shown in figure 8. An interesting observation is that co-ion depletion occurs at a very low potential for $[C_6(mim)_2](Tf_2N)_2$/PC, indicating the outstanding co-ion expulsion capability of PC. It is probably due to the fact that the strong adsorption of PC molecules on graphite, which occupy a large fraction of space in EDLs, weakens the association of cation–anion pairs and facilitates the exclusion of co-ions from EDLs. Although stronger co-ion expulsion is observed in $[C_6(mim)_2](Tf_2N)_2$/PC electrolytes, the differential capacitance is not obviously increased compared with $[C_6(mim)_2](Tf_2N)_2$/ACN electrolytes. This is possibly attributable to the fewer counter-ions accumulated in EDLs formed by $[C_6(mim)_2](Tf_2N)_2$/PC, therefore the net charges in EDLs of $[C_6(mim)_2](Tf_2N)_2$/ACN and $[C_6(mim)_2](Tf_2N)_2$/PC are similar to each other with respect to response of potential change, leading to comparable differential capacitance.

Although the conductivity of $[C_6(mim)_2](Tf_2N)_2$/ACN electrolytes is greatly enhanced, suggesting improved power density, the concern as to whether the presence of ACN will compromise the energy density of supercapacitors is still troubling. We calculated the energy densities (figure 9) as a function of absolute potential drop between the cathode and anode for supercapacitors with neat $[C_6(mim)_2](Tf_2N)_2$, $[C_6(mim)_2](Tf_2N)_2$/ACN and $[C_6(mim)_2](Tf_2N)_2$/PC as the electrolyte, respectively. The result demonstrates that the presence of the organic solvent ACN or PC in electrolytes does not reduce the stored energy density of supercapacitors compared with the neat IL electrolytes without organic solvents. Thus, adding organic solvents into DIL electrolytes of supercapacitors provides enhanced conductivity and charge/discharge rate without losing the energy density stored.

In summary, this work investigates the influence of the organic solvents ACN and PC on the conductivity of DIL electrolyte $[C_6(mim)_2](Tf_2N)_2$, their EDL structure and the *C–V* curve of $[C_6(mim)_2](Tf_2N)_2$-based supercapacitors using MD simulations. Greatly enhanced conductivity by the addition of ACN is observed in both MD and experimental measurements. There are more cations and anions in the EDLs of neat $[C_6(mim)_2](Tf_2N)_2$ than in those of $[C_6(mim)_2](Tf_2N)_2$/organic solvents. The presence of organic solvents is also found to facilitate the dissociation of cation–anion pairs in EDLs, leading to the expulsion of co-ions from EDLs at charged electrodes. PC exhibits outstanding co-ion expulsion capability due to its stronger adsorption on graphite in contrast to ACN. Furthermore, the bell-shaped *C–V* curve observed in the neat DIL-based supercapacitor becomes flattened in the DIL/ACN-based one and the capacitance is slightly increased due to the presence of ACN. A similar *C–V* curve was observed for DIL/PC. The cumulative number density in EDLs is used to explain the discrepancy of *C–V* curves of DIL- and

DIL/ACN-based supercapacitors. The energy density stored in the supercapacitor changes little with the presence of ACN or PC in the DIL electrolyte.

Besides all of the aforementioned advantages of using organic solvents as additives to DILs, the former can potentially reduce the cost of the DIL-based supercapacitors, which is crucial for commercial applications. For instance, ILs are relatively inexpensive to prepare on the small laboratory scale. However, the costs associated with their large-scale preparation, and at high purity, could make these costs unacceptable for commercialization. By using organic solvents such as ACN, which is already used in commercial supercapacitors, the increase in power and energy density granted by the DIL/ACN electrolytes can be achieved at a reasonable cost.

Acknowledgments

This work was supported by the Fluid Interface Reactions, Structures, and Transport (FIRST) Center, an Energy Frontier Research Center funded by the US Department of Energy, Office of Science, Office of Basic Energy Sciences. We acknowledge the National Energy Research Scientific Computing Center (NERSC), which is supported by the Office of Science of the US Department of Energy under Contract No DE-AC02-05CH11231. GF also appreciates the Palmetto cluster at Clemson University for providing computer time.

References

[1] Zhu Q, Song Y, Zhu X and Wang X 2007 Ionic liquid-based electrolytes for capacitor applications *J. Electroanal. Chem.* **601** 229–36

[2] Arbizzani C, Biso M, Cericola D, Lazzari M, Soavi F and Mastragostino M 2008 Safe, high-energy supercapacitors based on solvent-free ionic liquid electrolytes *J. Power Sources* **185** 1575–9

[3] Wishart J F 2009 Energy applications of ionic liquids *Energy Environ. Sci.* **2** 956–61

[4] Anderson J L, Ding R F, Ellern A and Armstrong D W 2005 Structure and properties of high stability geminal dicationic ionic liquids *J. Am. Chem. Soc.* **127** 593–604

[5] Shirota H, Mandai T, Fukazawa H and Kato T 2011 Comparison between dicationic and monocationic ionic liquids: liquid density, thermal properties, surface tension, and shear viscosity *J. Chem. Eng. Data* **56** 2453–9

[6] Zhu Y W *et al* 2011 Carbon-based supercapacitors produced by activation of graphene *Science* **332** 1537–41

[7] Tokuda H, Baek S J and Watanabe M 2005 Room-temperature ionic liquid–organic solvent mixtures: conductivity and ionic association *Electrochemistry* **73** 620–2

[8] Arulepp M, Permann L, Leis J, Perkson A, Rumma K, Janes A and Lust E 2004 Influence of the solvent properties on the characteristics of a double layer capacitor *J. Power Sources* **133** 320–8

[9] Lin R, Taberna P L, Chmiola J, Guay D, Gogotsi Y and Simon P 2009 Microelectrode study of pore size, ion size, and solvent effects on the charge/discharge behavior of microporous carbons for electrical double-layer capacitors *J. Electrochem. Soc.* **156** A 7–12

[10] Cho W J, Yeom C G, Kim B C, Kim K M, Ko J M and Yu K H 2013 Supercapacitive properties of activated carbon electrode in organic electrolytes containing single- and double-cationic liquid salts *Electrochim. Acta* **89** 807–13

[11] Guerfi A, Dontigny M, Charest P, Petitclerc M, Lagacé M, Vijh A and Zaghib K 2010 Improved electrolytes for Li-ion batteries: mixtures of ionic liquid and organic electrolyte with enhanced safety and electrochemical performance *J. Power Sources* **195** 845–52

[12] Diaw M, Chagnes A, Carre B, Willmann P and Lemordant D 2005 Mixed ionic liquid as electrolyte for lithium batteries *J. Power Sources* **146** 682–4

[13] Yu Z, Vlachopoulos N, Hagfeldt A and Kloo L 2013 Incompletely solvated ionic liquid mixtures as electrolyte solvents for highly stable dye-sensitized solar cells *RSC Adv.* **3** 1896–901

[14] Chaban V V, Voroshyloya I V, Kalugin O N and Prezhdo O V 2012 Acetonitrile boosts conductivity of imidazolium ionic liquids *J. Phys. Chem.* B **116** 7719–27

[15] Van Aken K L, McDonough J K, Li S, Feng G, Chathoth S M, Mamontov E, Fulvio P F, Cummings P T, Dai S and Gogotsi Y 2014 Effect of cation on diffusion coefficient of ionic liquids at onion-like carbon electrodes *J. Phys.:Condens. Matter* **26** 284104

[16] Feng G, Huang J S, Sumpter B G, Meunier V and Qiao R 2010 Structure and dynamics of electrical double layers in organic electrolytes *Phys. Chem. Chem. Phys.* **12** 5468–79

[17] Merlet C, Salanne M, Rotenberg B and Madden P A 2013 Influence of solvation on the structural and capacitive properties of electrical double layer capacitors *Electrochim. Acta* **101** 262–71

[18] Feng G, Huang J S, Sumpter B G, Meunier V and Qiao R 2011 A 'counter-charge layer in generalized solvents' framework for electrical double layers in neat and hybrid ionic liquid electrolytes *Phys. Chem. Chem. Phys.* **13** 14723–34

[19] Jiang D E, Jin Z H, Henderson D and Wu J Z 2012 Solvent effect on the pore-size dependence of an organic electrolyte supercapacitor *J. Phys. Chem. Lett.* **3** 1727–31

[20] Kurzweil P 2009 Capacitors: electrochemical double-layer capacitors *Encyclopedia of Electrochemical Power Sources* ed J Garche (Amberg: Elsevier) vol 1 p 607

[21] Yeganegi S, Soltanabadi A and Farmanzadeh D 2012 Molecular dynamic simulation of dicationic ionic liquids: effects of anions and alkyl chain length on liquid structure and diffusion *J. Phys. Chem.* B **116** 11517–26

[22] Lopes J N C, Deschamps J and Padua A A H 2004 Modelling ionic liquids using a systematic altatom force field *J. Phys. Chem*. B **108** 2038–47

[23] Nikitin A M and Lyubartsev A P 2007 New six-site acetonitrile model for simulations of liquid acetonitrile and its aqueous mixtures *J. Comput. Chem.* **28** 2020–6

[24] Wang J M, Wolf R M, Caldwell J W, Kollman P A and Case D A 2004 Development and testing of a general amber force field *J. Comput. Chem.* **25** 1157–74

[25] Yang L, Fishbine B H, Migliori A and Pratt L R 2010 Dielectric saturation of liquid propylene carbonate in electrical energy storage applications *J. Chem. Phys.* **132** 044701

[26] Cornell W D, Cieplak P, Bayly C I, Gould I R, Merz K M, Ferguson D M, Spellmeyer D C, Fox T, Caldwell J W and Kollman P A 1995 A second generation force field for the simulation of proteins, nucleic acids, and organic molecules *J. Am. Chem. Soc.* **117** 5179–97

[27] Hess B, Bekker H, Berendsen H J C and Fraaije J G E M 1997 Lincs: a linear constraint solver for molecular simulations *J. Comput. Chem.* **18** 1463–72

[28] Essmann U, Perera L, Berkowitz M L, Darven T, Lee H and Pederson LG 1995 A smooth particle mesh & wald method *J. Chem. Phys*. **103** 8577–93

[29] Yeh I C and Berkowitz M L 1999 Ewald summation for systems with slab geometry *J. Chem. Phys.* **111** 3155–62

[30] Berendsen H J C, Vanderspoel D and Vandrunen R 1995 Gromacs—a message-passing parallel molecular-dynamics implementation *Comput. Phys. Commun.* **91** 43–56

[31] Schröder C, Haberler M and Steinhauser O 2008 On the computation and contribution of conductivity in molecular ionic liquids *J. Chem. Phys.* **128** 134501

[32] Li S, Van Aken K L, McDonough J K, Feng G, Gogotsi Y and Cummings P T 2013 The electrical double layer of dicationic ionic liquids at onion-like carbon surface *J. Phys. Chem.* C **118** 3901–9

[33] Fedorov M V and Kornyshev A A 2008 Towards understanding the structure and capacitance of electrical double layer in ionic liquids *Electrochim. Acta* **53** 6835–40